Structure of ^{36}Ca under the Coulomb Magnifying Glass

L. Lalanne,[1,2,*] O. Sorlin,[2,†] A. Poves,[3] M. Assié,[1] F. Hammache,[1] S. Koyama,[4,2] D. Suzuki,[5] F. Flavigny,[6] V. Girard-Alcindor,[2] A. Lemasson,[2] A. Matta,[6] T. Roger,[2] D. Beaumel,[1] Y. Blumenfeld,[1] B. A. Brown,[7] F. De Oliveira Santos,[2] F. Delaunay,[6] N. de Séréville,[1] S. Franchoo,[1] J. Gibelin,[6] J. Guillot,[1] O. Kamalou,[2] N. Kitamura,[8] V. Lapoux,[9] B. Mauss,[5,2] P. Morfouace,[2,10] M. Niikura,[4] J. Pancin,[2] T. Y. Saito,[4] C. Stodel,[2] and J-C. Thomas[2]

[1]*Université Paris-Saclay, CNRS/IN2P3, IJCLab, 91405 Orsay, France*
[2]*Grand Accélérateur National d'Ions Lourds (GANIL), CEA/DRF-CNRS/IN2P3, Bd. Henri Becquerel, 14076 Caen, France*
[3]*Departamento de Física Teórica and IFT-UAM/CSIC, Universidad Autónoma de Madrid, E-2804 Madrid, Spain*
[4]*Department of Physics, University of Tokyo, 113-0033, Tokyo, Japan*
[5]*RIKEN Nishina Center, 2-1, Hirosawa, Wako, Saitama 351-0198, Japan*
[6]*Normandie Université, ENSICAEN, UNICAEN, CNRS/IN2P3, LPC Caen, 14000 Caen, France*
[7]*Department of Physics and Astronomy, National Superconducting Cyclotron Laboratory, Michigan State University, East Lansing, Michigan, USA*
[8]*Center for Nuclear Study, University of Tokyo, 113-0033, Tokyo, Japan*
[9]*CEA, Centre de Saclay, IRFU, Service de Physique Nucléaire, 91191 Gif-sur-Yvette, France*
[10]*CEA, DAM, DIF, F-91297 Arpajon, France*

(Received 7 December 2021; revised 5 May 2022; accepted 8 August 2022; published 15 September 2022)

Detailed spectroscopy of the neutron-deficient nucleus ^{36}Ca was obtained up to 9 MeV using the ^{37}Ca$(p,d)^{36}$Ca and the ^{38}Ca$(p,t)^{36}$Ca transfer reactions. The radioactive nuclei, produced by the LISE spectrometer at GANIL, interacted with the protons of the liquid hydrogen target CRYPTA, to produce light ejectiles (the deuteron d or triton t) that were detected in the MUST2 detector array, in coincidence with the heavy residues identified by a zero-degree detection system. Our main findings are (i) a similar shift in energy for the 1_1^+ and 2_1^+ states by about -250 keV, as compared with the mirror nucleus ^{36}S; (ii) the discovery of an intruder 0_2^+ state at 2.83(13) MeV, which appears below the first 2^+ state, in contradiction with the situation in ^{36}S; and (iii) a tentative 0_3^+ state at 4.83(17) MeV, proposed to exhibit a bubble structure with two neutron vacancies in the $2s_{1/2}$ orbit. The inversion between the 0_2^+ and 2_1^+ states is due to the large mirror energy difference (MED) of $-516(130)$ keV for the former. This feature is reproduced by shell model calculations, using the sd-pf valence space, predicting an almost pure intruder nature for the 0_2^+ state, with two protons (neutrons) being excited across the $Z = 20$ magic closure in ^{36}Ca (^{36}S). This mirror system has the largest MEDs ever observed, if one excludes the few cases induced by the effect of the continuum.

DOI: 10.1103/PhysRevLett.129.122501

Introduction.—The studies of fundamental symmetries and the mechanisms that induce their breaking are crucial to the understanding and appreciation of the wealth of the physics processes ruling our world [1,2]. In atomic nuclei, the isospin symmetry is born out of the charge independence of the strong interaction which considers that protons and neutrons are two representations of the same particle, the nucleon. The electromagnetic interaction violates this symmetry and is the main mechanism responsible for isospin symmetry breaking effects (ISB). However, even if the Coulomb contribution to the total binding energy of the nucleus is quite large, it barely affects its spectroscopic properties, and energy-level schemes of mirror nuclei (with interchanged numbers of protons and neutrons) are generally found to be nearly identical.

ISB are known to produce small differences in the excitation energies of analog states in a pair of mirror nuclei, which are dubbed mirror energy differences (MEDs) [3–5]. The difference in $E2$ transition matrix elements between mirror nuclei has also been used as a probe of ISB; see, e.g., Refs. [6–8]. The Coulomb repulsion among the protons is the main source of MED. Its amplitude is generally small (10–100 keV) and very rarely exceeds ± 200 keV [9]. However, even a small MED of only a few tens of keV can produce quite a prominent effect, such as different ground-state spin values between the mirror pair ^{73}Sr-^{73}Br [10], commented in Refs. [9,11]. The study of MED probes in a unique manner the wave function of the nucleons inside the nucleus. Remarkable examples are (i) the evolution of MED along rotational bands, which yields insight into the changes in spatial correlations and spin alignment [12–14]; (ii) the large MED of up to 700 keV observed in the $A = 13$ (^{13}C-^{13}N) [4,5] and $A = 16$ (^{16}N-^{16}F) mirror pairs [15], also called Thomas-Ehrmann (TE) shifts, which probes the spatial expansion of

 © 2022 American Physical Society

unbound s orbits and the influence of the continuum; (iii) the persistence of mirror symmetry in the disappearance of the magic number 8 between ^{12}O and its partner ^{12}Be [16,17]; and (iv) a proposed change of shape between the mirror nuclei ^{70}Kr and ^{70}Se [6], based on $E2$ reduced transition matrix elements, which is however questioned in Ref. [18].

In the present work, we provide for the first time evidence of very large MED in conjunction with the phenomenon of shape coexistence through the experimental and theoretical studies of the 0_2^+, 2_1^+, and 1_1^+ states in the $A = 36$, $T = 2$ mirror pair, ^{36}S and ^{36}Ca. Note that these states are not subject to TE shifts as the Coulomb barrier of ^{36}Ca ($\simeq 6.1$ MeV) is much higher than the one- and two-proton emission thresholds ($\simeq 2.6$ MeV and 2.68 MeV, respectively).

Experimental techniques.—The ^{37}Ca and ^{38}Ca nuclei were produced at about 50 MeV/nucleon by fragmentation reactions of a 95 MeV/nucleon $^{40}Ca^{20+}$ beam, with an average intensity of ~ 2 μAe, in a 2-mm thick ^{9}Be target. They were selected through two different settings of the LISE3/GANIL spectrometer [19], leading to a purity of 20% and mean rates of 3×10^3 pps and 2×10^4 pps, respectively. They were subsequently tracked by two low-pressure multiwire detectors, CATS [20], before interacting with protons of a cryogenic liquid hydrogen target CRYPTA [21] (of effective thickness of 9.7 mg cm^{-2}). They were unambiguously identified by means of their time-of-flight (TOF) measurement between the CATS detectors and the cyclotron radio frequency.

The outgoing ions were detected by a zero-degree detection (ZDD) system, composed of an ionization chamber, yielding their Z identification, a set of two XY drift chambers, used to determine their outgoing angles, and a thick plastic scintillator, mostly used for time-of-flight measurements. The energy and angle of the light outgoing particles, either d or t from the transfer reactions, as well as proton(s) emitted from unbound states, were measured by a set of six MUST2 telescopes [22], each composed of a first stage of a 300-μm thick double-sided Silicon strip detector (DSSSD) and a second stage of sixteen 4-cm thick CsI crystals. Light particle identification was performed using the correlation between the energy loss, ΔE, and the residual energy, E, measured in the DSSSD and the CsI crystals, respectively (see Refs. [23,24] for more details).

Results.—The excitation energy E_x of ^{36}Ca was obtained from the $^{37}\mathrm{Ca}(p,d)^{36}\mathrm{Ca}$ [$^{38}\mathrm{Ca}(p,t)^{36}\mathrm{Ca}$] reactions using the missing mass method after gating on an incoming ^{37}Ca [^{38}Ca] in CATS and on a d [t] particle in MUST2. The total excitation energy spectrum obtained using the (p,d) reaction and gated on outgoing Ca, K, and Ar isotopes (using the ZDD) is shown in Fig. 1(a). The spectra obtained from the (p,t) reaction, gated only on outgoing Ca or only Ar, are shown in Figs. 1(c) and 1(d), respectively.

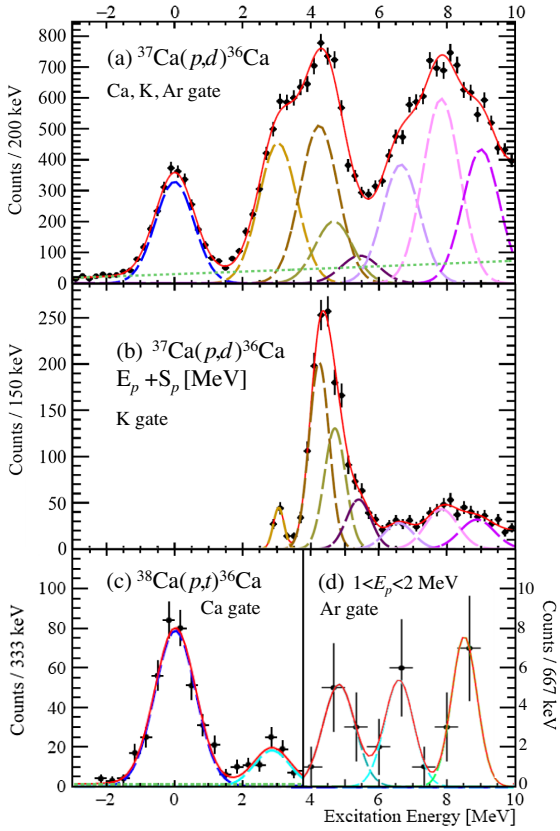

FIG. 1. (a) Excitation energy spectrum E_x of ^{36}Ca obtained from the (p,d) transfer reaction with a gate on outgoing Ca, K, and Ar. (b) One-proton energy spectrum [to which $S_p(^{36}\mathrm{Ca}) = 2599.6(61)$ keV has been added] obtained from the (p,d) reaction with a gate on outgoing K isotopes. E_x spectrum from the (p,t) reaction and gated on outgoing Ca is shown in (c), while the one in (d) is gated on outgoing Ar and the detection of one proton with a center-of-mass energy between 1 and 2 MeV. Individual contributions to the fits are shown with different color codes.

Figure 1(b) shows the one-proton energy reconstructed in the center of mass of ^{36}Ca using the (p,d) reaction with a gate on outgoing K only. Since the energy resolution reconstructed with the protons is better than with the deuterons ([23,24]), Fig. 1(b) allows the determination of the energy peak centroids to be used for the fit of Fig. 1(a) in the 4–5.5 MeV excitation energy range.

The red lines in Figs. 1(a)–1(d) display the best fits obtained using multiple Gaussian functions (shown with colored dotted lines) plus a small background contribution (green dashed line), generated by interactions of the beam particles with the windows of the LH_2 target, determined in a dedicated run with an empty target. The width of each peak used in the fit is constrained by simulations performed with the nptool package [25], the reliability of which is checked from the observed widths of isolated peaks [e.g., 0_1^+ at 0 MeV in Fig. 1(a) and 2_1^+ at 3 MeV in Fig. 1(b)]. A typical energy resolution in E_x of about 550 keV is found

for the peaks of Figs. 1(a), 1(c) and 1(d). The resolution in proton energy varies from 130 keV at 3 MeV to 500 keV at 8 MeV in Fig. 1(b). The number of contributions used in the fit was guided by the statistical tests of the χ^2 and the p value, as well as the number of states populated in the quasimirror reaction ^{37}Cl$(d,{}^3$He$)^{36}$S [26]. Finally, contributions of the one- and two-proton phase spaces have been found to be of less than 2% for excitation energies below 10 MeV (see Sec. 1 in the Supplemental Material [27]).

The differential cross sections corresponding to the ^{37}Ca$(p,d)^{36}$Ca and ^{38}Ca$(p,t)^{36}$Ca transfer reactions are shown in Figs. 2(a)–2(d) and 2(e)–2(f), respectively. They have been obtained by fitting the excitation energy spectra of Figs. 1(a) and 1(c) (with centroid values fixed at the energies measured using the full angular range) with slices of center-of-mass angles. A proper normalization of their amplitudes is made using the number of incident nuclei and the density of target protons, as well as taking into account the geometrical and detection efficiencies of the experimental setup. The shape of the distributions gives clear information on the transferred angular momentum L. Their amplitudes allow, when compared with the distorted wave born approximation (DWBA) calculations, for the determination of the neutron spectroscopic factor C^2S values for the (p,d) reaction, which are discussed first.

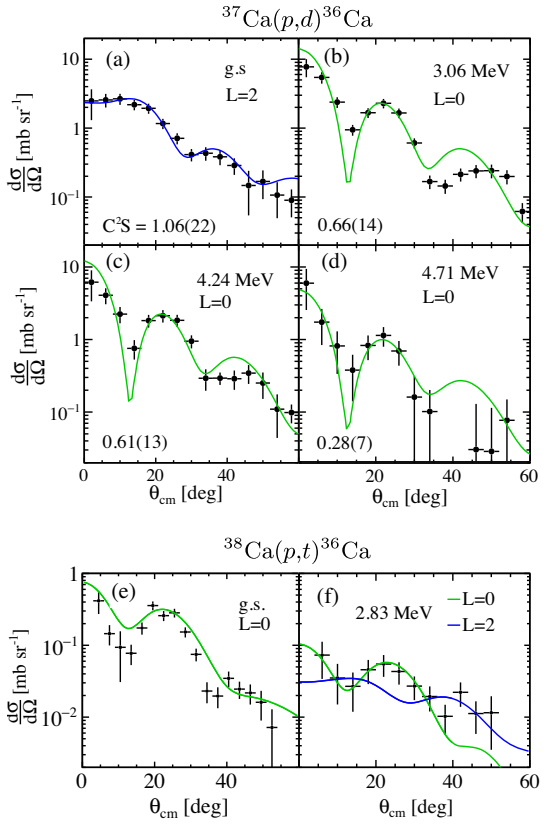

FIG. 2. Differential cross sections of the states identified in ^{36}Ca using the ^{37}Ca$(p,d)^{36}$Ca and ^{38}Ca$(p,t)^{36}$Ca transfer reactions are shown in (a)–(d) and (e),(f), respectively. (a)–(d) Blue (green) full lines show the results of the $L=2$ ($L=0$) DWBA calculations fitted to the data. (e),(f) Green and blue full lines correspond to results of the DWBA plus TNA calculations assuming $L=0$ and $L=2$ transfers, respectively. Panel (e) used TNA values directly extracted from the present shell-model calculations, while (f) is a result of fitted values (see text for details).

DWBA calculations have been performed with the code FRESCO [34] using the optical parameters given in Sec. 2 of the Supplemental Material [27]. For ^{37}Ca$(p,d)^{36}$Ca, three successive angular distribution patterns are clearly identified as a function of increasing E_x: $L=2$ for the ground state (g.s.) [Fig. 2(a)]; $L=0$ for the three states at $E_x=3.06(2)$, 4.24(4), and 4.71 (9) MeV [Figs. 2(b)–2(d)]; and $L=2$ for the four peaks at $E_x=5.41$, 6.54, 7.84, and 9.01 MeV (see Fig. 2 of Sec. 3 in the Supplemental Material [27]). These distributions likely correspond to the removal of neutrons in ^{37}Ca from the $1d_{3/2}$, $2s_{1/2}$, and $1d_{5/2}$ orbitals, leading to a sequence of expected $J^\pi=0^+$, (1^+ or 2^+), and (1^+ -4^+) states, respectively.

Spectroscopic factors, the uncertainties of which are dominated by the systematic error induced by the choice of optical potential parameters, are given in Table I. A C^2S value of 1.06(22) is found for the g.s., in excellent agreement with the value of 1.06 found in the mirror reaction [26] (see Table I). Within the error bars, it corresponds to the occupancy of the $1d_{3/2}$ orbital by about one neutron (proton) in ^{37}Ca (^{37}Cl). For the 2_1^+, 1^+, and 2_2^+ excited states, C^2S values of 0.66(14), 0.61(13), and 0.28(7) have been found, respectively, also fully compatible with those obtained in the mirror reaction. With these three states, a large fraction of the $2s_{1/2}$ strength, $C^2S=1.55(34)$, has been collected. At higher excitation energy, an integrated summed C^2S value of 4.38(88) has been obtained from 5 to 9.5 MeV (see Fig. 2 of Sec. 3 in the Supplemental Material [27]), to be compared to the full occupancy of the $1d_{5/2}$ orbital by six neutrons.

In the ^{38}Ca$(p,t)^{36}$Ca reaction, two states are observed in Fig. 1(c), gated on Ca in the ZDD: the 0^+ g.s. of ^{36}Ca, as well as an excited state at 2.83(13) MeV. Figures 2(e) and 2(f) show the corresponding differential cross sections. The two-nucleon amplitudes (TNA) have been computed using shell model calculations with configuration interaction (SM CI) [36], for a transition from the g.s. of ^{38}Ca to the 0_1^+, as well as to a 0_2^+ or 2_1^+ excited state in ^{36}Ca. These TNA, given in Sec. 4 of the Supplemental Material [27], have been used to perform DWBA calculations which are compared to experimental differential cross sections. As shown in Fig. 2(e), an excellent agreement is obtained for the ground state with an $L=0$ shape, which is the only possibility for a $0^+\rightarrow 0^+$ transition. The TNA that contributes by far the most to the reaction is the one arising from the removal of a pair of neutrons from the $1d_{3/2}$ orbital.

The shape of the angular distribution [Fig. 2(f)] of the 2.83(13) MeV state is much better fitted as well when

TABLE I. Summary of the experimental results and shell-model calculations for the ^{36}Ca-^{36}S mirror pair states with their proposed J^π values, excitation energy E_x in MeV, neutron [proton] spectroscopic factor values C^2S from the (p, d) [$(d, {}^3\mathrm{He})$] reaction and MED in keV. The C^2S of the 0_1^+ state is obtained when assuming a neutron removal from the $d_{3/2}$ orbital, while for the 2_1^+, 1^+, and 2_2^+ states a removal from the $s_{1/2}$ orbital is assumed. The last column shows the fraction of the wave function corresponding to the $0p-0h$ and $2p-2h$ configurations, according to the SM CI calculations.

	^{36}Ca present work				^{36}S						
	Exp.		Th.		Exp. [26]		Th.		MED		
J^π	E_x	C^2S	E_x	C^2S	E_x	C^2S	E_x	C^2S	Exp.	Th.	$0p-0h/2p-2h$
0^+	0.0	1.06(22)	0.0	0.91	0.0	1.06	0.0	0.93			0.92/0.08
0_2^+[a,b]	2.83(13)		2.70	≃0.0	3.346		3.42	≃0.0	−516(130)	−720	0.06/0.82
2_1^+	3.06(2)	0.66(14)	2.95	1.01	3.291	0.86(17)	3.25	1.09	−245(2)[c]	−300	0.79/0.20
1_1^+	4.24(4)	0.61(13)	4.00	0.71	4.523	0.75(15)	4.22	0.72	−280(41)	−220	0.90/0.10
2_2^+	4.71(9)	0.28(7)	3.81	0.10	4.577	0.25(5)	4.54	0.05	+133(90)	−730	0.12/0.79
(0_3^+)[b]	4.83(17)		4.36	≃0.0			4.92	≃0.0		−560	0.87/0.12

[a]Its configuration in ^{36}Ca, according to the present SM CI calculations, is protons $(d_{5/2})^{6-0.24}$ $(s_{1/2})^{2-0.48}$ $(d_{3/2})^{4-1.42}$ $(f_{7/2})^{0+1.8}$ $(p_{3/2})^{0+0.21}$ $(p_{1/2})^{0+0.02}$ $(f_{5/2})^{0+0.1}$ and neutrons $(d_{5/2})^{6-0.71}$ $(s_{1/2})^{2-0.85}$ $(d_{3/2})^{0+1.56}$. The first term in each superscript represents the normal occupancy value of the orbit and the second, preceded by a "+" or "−" sign, represents its calculated excess or reduction.
[b]State observed in the ^{38}Ca$(p, t)^{36}$Ca reaction. The obtained TNA, as well as that of the g.s., are given in Sec. 4 of the Supplemental Material [27].
[c]Value computed using the most precise energy of $E_x = 3045(2)$ keV for the 2_1^+ of ^{36}Ca from Ref [35].

assuming an $L = 0$ ($\chi^2/\mathrm{ndf} = 2.2/8$ for a fit up to 40°, green line) rather than an $L = 2$ distribution ($\chi^2/\mathrm{ndf} = 13.1/8$, blue line). It provides strong evidence of the existence of a 0_2^+ state below the 2_1^+ state, although a small contribution of the 2_1^+, lower than 20%, could not be excluded.

Figure 1(d) has been obtained with a gate on outgoing Ar nuclei and $1 \le E_p^{\mathrm{c.m.}}(\mathrm{MeV}) \le 2$ to select states in ^{36}Ca that underwent a sequential $2p$ decay through the $1/2^+$ resonant state at 1.553(5) MeV in ^{35}K to the ^{34}Ar g.s. Three peaks can be clearly identified at 4.83(17), 6.60(14), and 8.52(15) MeV. The decay of the relatively low excitation energy 4.83(17) MeV state through this low-J resonance will be strongly favored only if the state has $J^\pi = 0^+$ or 1^+, as the decay can proceed through the emission of an $L = 0$ proton, contrary to the case of higher spin values. We tentatively propose a $J^\pi = 0_3^+$ assignment to the 4.83(17) MeV state as the two-neutron transfer cross section for the odd-J, 1^+ state, is predicted to be orders of magnitude lower. Moreover, a $J^\pi = 0_3^+$ state at 4.967 MeV has been strongly populated in the ^{36}Ar$(p, t)^{34}$Ar reaction, involving isotone nuclei [37].

Discussion.—The mirror pair nuclei ^{36}Ca-^{36}S have been calculated with the shell-model code Antoine [38] using the same valence space and interactions as in Ref. [36]. There, the nuclear, isospin conserving part is given by the *sdfpu*-mix interaction [39]. The two-body matrix elements of the Coulomb interaction are computed with harmonic oscillator wave functions with $\hbar\omega = 41A^{-1/3} - 25A^{-2/3}$. The Coulomb corrections to the single-particle energies are taken from the experimental spectra of the $A = 17$ and $A = 41$ mirror nuclei. Theoretical level schemes of the mirror nuclei are compared to experimental ones in Fig. 3. The spectroscopic factors (C^2S) for the (p, d) reaction are gathered in Table I.

Starting with ^{36}S, the correspondence between theory and experiment is very good (see Fig. 3). The 0_3^+ state, predicted at 4.92 MeV has not yet been observed experimentally. It is seen in the last column of Table I that all states have well-defined structures and, of the six lower states, two are calculated to be intruders.

The present experiment confirms the energy of the 2_1^+ state in ^{36}Ca [40,41], which is, using the precise value of Ref. [35], 245(2) keV lower than in ^{36}S. Populated by the (p, d) reaction, it has a large C^2S value with an $L = 0$ angular distribution pattern, pointing to a pure $1p1h$ configuration with a hole in the $2s_{1/2}$ orbital. The 1^+ state has a similar structure and experiences a similar shift of

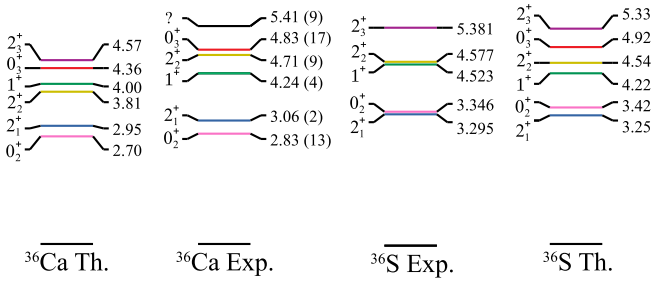

FIG. 3. Partial level scheme of the mirror pair ^{36}Ca-^{36}S obtained experimentally (Exp.) and from shell model calculations (Th.). Energy values for ^{36}Ca are those obtained in this Letter.

−280(41) keV. These shifts can be attributed to their reduction of $2s_{1/2}$ occupancy, as compared with the ground state. As protons in this orbital feel a smaller Coulomb repulsion than in the $d_{3/2}$ one, the 1^+, 2^+ excitation energies in ^{36}S are pushed upward with respect to ^{36}Ca. The calculated C^2S value of the 2_2^+ in the two mirror nuclei, predicted to be an intruder state, is 3–5 times smaller than the 2_2^+ experimental value. This points to an incorrect interpretation of its structure, which probably explains why experimental and calculated MEDs given in Table I disagree. It is not completely excluded that the observed state would be in reality the 2_3^+ (with the 2_2^+ state unobserved). Further experimental and theoretical investigations are needed to elucidate this point.

The largest MED shift is for the 0_2^+, which is observed in ^{36}Ca for the first time. As discussed in Ref. [36], its very large MED of −516(130) keV, comparable to the calculated value of −720 keV, is due to the addition of two contributions. The first comes from its $2p2h$ proton intruder nature, because the two protons promoted across $Z = 20$ in the pf shell feel less Coulomb repulsion than in the sd shell. Moreover, the opening of the proton core leads to an increase of the degree of collectivity and has a large influence on the neutron configuration, understood to be a $1p1h$ with one neutron missing in the $2s_{1/2}$ orbital, as for the $(2_1^+, 1^+)$ doublet. These two effects stem naturally from the occupancies (listed below Table I in footnote "a") and sum coherently to generate the very large observed MED.

Concerning the 0_3^+ state, its structure is predicted to be dominated by two neutron holes in the $2s_{1/2}$ orbital, which would result in a large central depletion similar to that described for protons in Ref. [42]. A Coulomb shift of −560 keV, twice as large as for the 2_1^+ and 1_1^+ states, is expected from the calculation. In ^{36}S an unobserved 0_3^+ state should be present around 4.9 MeV.

Summary.—The ^{37}Ca$(p,d)^{36}$Ca transfer reaction was used to populate the ground state of ^{36}Ca as well as the $(2_{1,2}^+, 1_1^+)$ states, through the removal of a neutron from the $1d_{3/2}$ and $2s_{1/2}$ orbitals, respectively. Their L assignments and C^2S values are deduced from the comparison between their experimental differential cross section and DWBA calculations. Very similar C^2S values were found with the quasimirror reaction ^{37}Cl$((d,{}^3\mathrm{He})^{36}$S for the states up to an excitation energy of 5 MeV, pointing to a very similar structure between the mirror states of ^{36}Ca and ^{36}S. The large observed MED, of about −250 keV for the 2_1^+ and 1_1^+ states, is understood as originating from their pure $1p1h$ structure, with one neutron (proton) less in the $2s_{1/2}$ orbital, as compared with the ground state. The ^{38}Ca$(p,t)^{36}$Ca reaction revealed the existence of a 0_2^+ state at 2.83(13) MeV, which would correspond to the ground state intruder configuration in ^{32}Ca, if mirror symmetry with ^{32}Mg would be preserved. This 0_2^+ experiences a spectacular MED of about −516(130) keV, which is interpreted by its combined neutron $1p1h$ and proton $2p2h$ intruder components. This amazingly large isospin-symmetry breaking is extremely rare in the chart of nuclides. It can be fully interpreted by the effect of the Coulomb interaction and is favored because of the shape coexistence between the two 0^+ states in ^{36}Ca. It makes the ^{36}Ca-^{36}S mirror pair a remarkable physics case in which the Coulomb interaction acts as a magnifying glass to probe their structures, without perturbing them.

The present work, together with the ground state properties of ^{36}Ca [43,44], is expected to serve as a benchmark case for *ab initio* calculations that are supposed to rigorously treat all ISB effects of the nuclear force. In the broader context of nuclear astrophysics (and in particular for the rapid proton-capture process), the present conclusions showing good symmetry in C^2S strengthen the validity of using the same C^2S values between mirror reactions, even when large MED are present, to determine unknown reaction cross sections.

The continued support of the staff of the GANIL facility is gratefully acknowledged. D. S. was supported by the JSPS KAKENHI Grant No. 19H01914. A. P.'s work is supported in part by the Ministerio de Ciencia, Innovación y Universidades (Spain), Grant No. CEX2020-001007-S funded by MCIN/AEI and Grant No. PGC-2018-94583. Support from the National Science Foundation Grant No. PHY-1811855 is also acknowledged.

*louis-alexandre.lalanne@cern.ch
†olivier.sorlin@ganil.fr

[1] T. D. Lee and C. N. Yang, Phys. Rev. **104**, 245 (1956).
[2] P. W. Higgs, Phys. Lett. **12**, 132 (1964).
[3] J. A. Nolen and J. P. Schiffer, Annu. Rev. Nucl. Sci. **19**, 471 (1969).
[4] R. G. Thomas, Phys. Rev. **81**, 148 (1951).
[5] J. B. Ehrman, Phys. Rev. **81**, 412 (1951).
[6] K. Wimmer *et al.*, Phys. Rev. Lett. **126**, 072501 (2021).
[7] A. Boso *et al.*, Phys. Lett. B **797**, 134835 (2019).
[8] M. M. Giles *et al.*, Phys. Rev. C **99**, 044317 (2019).
[9] J. Henderson and S. R. Stroberg, Phys. Rev. C **102**, 031303(R) (2020).
[10] D. E. M. Hoff *et al.*, Nature (London) **580**, 52 (2020).
[11] S. M. Lenzi, A. Poves, and A. O. Macchiavelli, Phys. Rev. C **102**, 031302(R) (2020).
[12] D. D. Warner, M. A. Bentley, and P. Van Isacker, Nat. Phys. **2**, 311 (2006).
[13] S. M. Lenzi *et al.*, Phys. Rev. Lett. **87**, 122501 (2001).
[14] M. A. Bentley *et al.*, Phys. Rev. Lett. **97**, 132501 (2006).
[15] I. Stefan *et al.*, Phys. Rev. C **90**, 014307 (2014).
[16] D. Suzuki *et al.*, Phys. Rev. Lett. **103**, 152503 (2009).
[17] D. Suzuki *et al.*, Phys. Rev. C **93**, 024316 (2016).
[18] S. M. Lenzi, A. Poves, and A. O. Macchiavelli, Phys. Rev. C **104**, L031306 (2021).

[19] R. Anne, D. Bazin, A. C. Mueller, J. C. Jacmart, and M. Langevin, Nucl. Instrum. Methods Phys. Res., Sect. A **257**, 215 (1987).
[20] S. Ottini-Hustache *et al.*, Nucl. Instrum. Methods Phys. Res., Sect. A **431**, 476 (1999).
[21] S. Koyama, D. Suzuki, M. Assié, N. Kitamura, L. Lalanne, M. Niikura, H. Otsu, T. Y. Saito, and O. Sorlin, Nucl. Instrum. Methods Phys. Res., Sect. A **1010**, 165477 (2021).
[22] E. Pollacco *et al.*, Eur. Phys. J. A **25**, 287 (2005).
[23] L. Lalanne *et al.*, Phys. Rev. C **103**, 055809 (2021).
[24] L. Lalanne, Ph.D. thesis, Université Paris-Saclay, 2021.
[25] A. Matta, P. Morfouace, N. de Séréville, F. Flavigny, M. Labiche, and R. Shearman, J. Phys. G **43**, 045113 (2016).
[26] W. S. Gray, P. J. Ellis, T. Wei, R. M. Polichar, and J. Jänecke, Nucl. Phys. **A140**, 494 (1970).
[27] See Supplemental Material at http://link.aps.org/supplemental/10.1103/PhysRevLett.129.122501 for Sec. 1, the phase space, which includes Refs. [26]; Sec. 2, the optical model parameters used for the (p,d) and (p,t) transfer reaction, which includes Refs. [29–34]; Sec. 3, the states originating from the neutron $d_{5/2}$ removal; and Sec. 4, the calculated TNA values values for the (p,t) transfer reaction.
[28] J. J. H. Menet, E. E. Gross, J. J. Malanify, and A. Zucker, Phys. Rev. C **4**, 1114 (1971).
[29] R. C. Johnson and P. C. Tandy, Nucl. Phys. **A235**, 56 (1974).
[30] F. D. Becchetti and G. W. Greenlees, Phys. Rev. **182**, 1190 (1969).
[31] A. N. Bohr and B. R. Mottelson, *Nuclear Structure* (World Scientific Publishing Company, Singapore, 1998).
[32] R. V. Reid, Ann. Phys. (N.Y.) **50**, 411 (1968).
[33] X. Li, C. Liang, and C. Cai, Nucl. Phys. **A789**, 103 (2007).
[34] I. J. Thompson, C. R. Phys. **7**, 167 (1988).
[35] A. M. Amthor, Ph.D. thesis, Michigan State University, 2009.
[36] J. J. Valiente-Dobon, A. Poves, A. Gadea, and B. Fernandez-Dominguez, Phys. Rev. C **98**, 011302(R) (2018).
[37] R. A. Paddock *et al.*, Phys. Rev. C **5**, 485 (1972).
[38] E. Caurier, G. Martínez-Pinedo, F. Nowacki, A. Poves, and A. P. Zuker, Rev. Mod. Phys. **77**, 427 (2005).
[39] E. Caurier, F. Nowacki, and A. Poves, Phys. Rev. C **90**, 014302 (2014).
[40] P. Doornenbal *et al.*, Phys. Lett. B **647**, 237 (2007).
[41] A. Bürger *et al.*, Phys. Rev. C **86**, 064609 (2012).
[42] A. Mutschler *et al.*, Nat. Phys. **13**, 152 (2017).
[43] A. J. Miller *et al.*, Nat. Phys. **15**, 432 (2019).
[44] J. Surbrook, G. Bollen, M. Brodeur, A. Hamaker, D. Pérez-Loureiro, D. Puentes, C. Nicoloff, M. Redshaw, R. Ringle, S. Schwarz, C. S. Sumithrarachchi, L. J. Sun, A. A. Valverde, A. C. C. Villari, C. Wrede, and I. T. Yandow, Phys. Rev. C **103**, 014323 (2021).